University of Glasgow

Longo, W. M. et al. (2018) Widespread occurrence of distinct alkenones from Group I haptophytes in freshwater lakes: implications for paleotemperature and paleoenvironmental reconstructions. *Earth and Planetary Science Letters*, 492, pp. 239-250. (doi:10.1016/j.epsl.2018.04.002)

This is the author's final accepted version.

There may be differences between this version and the published version. You are advised to consult the publisher's version if you wish to cite from it.

http://eprints.gla.ac.uk/160781/

Deposited on: 17 April 2018

Enlighten – Research publications by members of the University of Glasgow
http://eprints.gla.ac.uk

Widespread occurrence of distinct alkenones from Group I haptophytes in freshwater lakes: Implications for paleotemperature and paleoenvironmental reconstructions

William M. Longo*[1,2]; Yongsong Huang*[1,3]; Yuan Yao[3]; Jiaju Zhao[3]; Anne E. Giblin[4]; Xian Wang[1]; Roland Zech[5]; Torsten Haberzettl[5]; Ludwig Jardillier[6]; Jaime Toney[7]; Zhonghui Liu[8]; Sergey Krivonogov[9,10]; Marina Kolpakova[9]; Guoqiang Chu[11]; William J. D'Andrea[12]; Naomi Harada[13]; Kana Nagashima[13]; Miyako Sato[13]; Hitoshi Yonenobu[14]; Kazuyoshi Yamada[15]; Katsuya Gotanda[16]; Yoshitsugu Shinozuka[17]

[1]Department of Earth, Environmental and Planetary Sciences, Brown University, 324 Brook St., Providence, RI 02912, USA
[2]*Current Address*: Department of Marine Chemistry and Geochemistry, Woods Hole Oceanographic Institution, 266 Woods Hole Rd., Woods Hole, MA 02543, USA
[3]Institute of Earth Environment, Chinese Academy of Sciences, Shaanxi PR, China
[4]The Ecosystems Center, Marine Biological Laboratory, 7 MBL St., 02543Woods Hole, MA, USA
[5]Institute of Geography, Friedrich-Schiller-University Jena, 07745 Jena, Germany
[6]Unite´ d'Ecologie, Systématique et Evolution, CNRS UMR 8079, Université Paris-Sud, 91405 Orsay, France
[7]Department of Geographical and Earth Sciences, University of Glasgow, Scotland
[8]Department of Earth Sciences, The University of Hong Kong, Hong Kong
[9]Institute of Geology and Mineralogy SB RAS, Novosibirsk 630090, Russia
[10]Novosibirsk State University, Novosibirsk 630090, Russia
[11]Institute of Geology and Geophysics, Chinese Academy of Sciences, Beijing PR, China
[12]Lamont-Dohery Earth Observatory, Columbia University, New York, New York, USA
[13]Japan Agency for Marine-Earth Science and Technology, Yokosuka 237-0061, Japan
[14]College of Education, Naruto University of Education, Naruto 772-8502, Japan
[15]Museum of Natural and Environmental history, Shizuoka 422-8017, Japan
[16]Chiba University of Commerce, Chiba 272-8512, Japan
[17]Ritsumeikan University, Kyoto 603-8577, Japan

* Corresponding Authors:

William M. Longo
E-mail: wlongo@whoi.edu
Tel: +1 508 289 2821

Yongsong Huang
E-mail: yongsong_huang@brown.edu
Tel: +1 401 863 3822
Fax: +1 401 863 2058

Abstract

Alkenones are C_{35} – C_{42} polyunsaturated ketone lipids that are commonly employed to reconstruct changes in sea surface temperature. However, their use in coastal seas and saline lakes can be hindered by species-mixing effects. We recently hypothesized that freshwater lakes are immune to species-mixing effects because they appear to exclusively host Group I haptophyte algae, which produce a distinct distribution of alkenones with a relatively consistent response of alkenone unsaturation to temperature. To evaluate this hypothesis and explore the geographic extent of Group I haptophytes, we analyzed alkenones in sediment and suspended particulate matter samples from lakes distributed throughout the mid- and high latitudes of the Northern Hemisphere (n=30). Our results indicate that Group I-type alkenone distributions are widespread in freshwater lakes from a range of different climates (mean annual air temperature range: -17.3—10.9 °C; mean annual precipitation range: 125—1657 mm $year^{-1}$; latitude range: 40—81 °N), and are commonly found in neutral to basic lakes (pH>7.0), including volcanic lakes and lakes with mafic bedrock. We show that these freshwater lakes do not feature alkenone distributions characteristic of Group II lacustrine haptophytes, providing support for the hypothesis that freshwater lakes are immune to species-mixing effects. In lakes that underwent temporal shifts in salinity, we observed mixed Group I/II alkenone distributions and the alkenone contributions from each group could be quantified with the RIK_{37} index. Additionally, we observed significant correlations of alkenone unsaturation (U^{K}_{37}) with seasonal and mean annual air temperature with this expanded freshwater lakes dataset, with the strongest correlation occurring during the spring transitional season ($U^{K}_{37} = 0.029*T - 0.49$; $r^2 = 0.60$; $p < 0.0001$). We present new sediment trap data from two lakes in northern Alaska (Toolik Lake, 68.632 °N, 149.602 °W; Lake E5, 68.643 °N, 149.458 °W) that demonstrate the highest sedimentary fluxes

of alkenones in the spring transitional season, concurrent with the period of lake ice melt and isothermal mixing. Together, these data provide a framework for evaluating lacustrine alkenone distributions and utilizing alkenone unsaturation as a spring lake temperature proxy in freshwater lakes.

Key Words

Alkenones; Paleoclimate; Paleoenvironment; Temperature Proxy; Freshwater Lakes; Chemotaxonomy

1. Introduction

Long-chain alkenones (LCAs) are C_{35} – C_{42} aliphatic unsaturated ketones that are produced by a relatively limited number of species from the Isochrysidales order of Haptophyte algae. LCAs are globally distributed in oceans, estuaries and inland lakes. They have been studied extensively because the degree of LCA unsaturation is well correlated with the temperature of the water in which the lipids are produced, providing the basis for the widely used U^{K}_{37} and $U^{K'}_{37}$ temperature proxies (Brassell et al., 1986; Prahl and Wakeham, 1987).

In the global oceans, LCA production is dominated by two closely related haptophyte species – *Emiliania huxleyi* and *Gephyrocapsa oceanica* (Volkman et al., 1980; Volkman et al., 1995; Conte et al., 1998) – that are phylogenetically classified as Group III haptophytes (Theroux et al., 2010). Algal cultures of various strains of these organisms demonstrated that the temperature sensitivity of LCA unsaturation could vary as a function of the producing species (Prahl and Wakeham, 1987; Volkman et al., 1995). However, global core-top and water column calibrations of $U^{K'}_{37}$ vs. sea surface temperature (SST) indicated that temperature exerts a strong first-order control on the index in most open marine settings (Müller et al., 1998; Conte et al., 2006). This suggests that changes in species composition – defined here as "species effects" – generally do not impair marine SST reconstructions.

Coastal seas, estuaries and lakes, however, contain several different species of LCA-producing haptophyte algae that collectively exhibit more genetic diversity than their open marine relatives (Coolen et al., 2004; D'Andrea et al., 2006; Theroux et al., 2010; Bendif et al., 2013). Different haptophyte species often display disparate temperature sensitivities and LCA distributions (Prahl

et al., 1988; Volkman et al., 1995; Sun et al., 2007; Ono et al., 2012; Nakamura et al., 2014; D'Andrea et al., 2016; Longo et al., 2016; Nakamura et al., 2016), which have caused species effects on LCA-based temperature reconstructions in saline lakes and coastal waters (Randlett et al., 2014; Wang et al., 2015, Warden et al., 2016). The diversity of LCA-producing haptophytes in these environments necessitates that species effects and associated ecological factors (e.g., production seasonality) be accounted for before LCA-based temperature reconstructions are pursued (e.g. Wang et al., 2015).

Recent observations have suggested that LCAs from freshwater lakes feature distinct distributions (Longo et al., 2016; Song et al., 2016b) and are produced by a specific phylogenetic clade of haptophyte algae – the so-called Group I phylotype (D'Andrea et al., 2006; Theroux et al., 2010; Longo et al., 2016). Group I haptophyte species have yet to be physically described, however genetic and geochemical data have shown that these organisms produce a highly specific LCA distribution (Longo et al., 2013; Dillon et al., 2016) with a narrow range of temperature sensitivities across sites (D'Andrea et al., 2016; Longo et al., 2016). These findings prompted the hypotheses that freshwater lakes are potentially immune to species effects and furthermore, that new LCA indices involving the Group I-specific tri-unsaturated isomeric LCAs (RIK_{37} and RIK_{38E}) could be used to identify and quantify species mixing in sedimentary records (Longo et al., 2016). These indices would thereby establish metrics to assess the validity of LCA-based temperature estimations and concurrently reconstruct salinity-induced shifts in haptophyte species assemblages. Longo et al. (2016) introduced and provided support for these hypotheses from a number of Arctic lakes in northern Alaska, yet they remain to be tested on a larger scale. Here, we address these hypotheses by investigating LCA distributions in sediments

and suspended particulate matter (SPM) samples from lakes distributed throughout the mid- to high latitudes of the Northern Hemisphere. Concurrently, we provide an assessment of LCA occurrence, temperature sensitivity and production seasonality in freshwater lakes.

2. Methods

2.1. Samples and sample preparation

Samples were obtained from a number of sources including SPM, sediment traps, surface sediments and archived sediment cores (Fig 1; Tables 1, S1).

2.1.1. Suspended particulate matter

SPM samples were collected from Lake Ichino-megata, Japan (39.96 °N, 139.74 °E) on May 1, 2013 (G-09) and June 1, 2013 (G-10) by filtration of lake water (20 L) through glass fiber (GF/F) filters. Filters were freeze-dried and lipids were extracted with dichloromethane:methanol (9:1; v/v) using an automated solvent extraction system (100 °C and 1500 psi). The extracts were saponified in 0.5 mol L^{-1} KOH in methanol at 80 °C for 2 h. The neutral fraction was separated into sub-fractions by silica-gel column chromatography using an automated sample preparation system (Rapid Trace SPE Workstation, Zymark Corp., Hopkinton, MA, USA). The solvents and sub-fractionation steps were the same as described previously (Harada et al., 2003). SPM samples were processed at the Japan Agency for Marine-Earth Science and Technology and shipped to Brown University, USA for LCA analysis.

2.1.2. Surface sediments and archived sediment core and sediment trap samples

Surface sediments were collected from lakes in Northeastern China, Germany, France, Japan and Inner Mongolia. Surface sediments were collected as the top 0-1 or 0-2 cm of sediment obtained from sediment cores collected by gravity or pole coring devices, or as Ekman grab samples. Whenever possible, sediment samples were collected from the deepest point in the lake, in order to provide an integrated signal of water column LCA production. Sediments were freeze-dried

and shipped to Brown University for further processing. Extraction and purification were carried out using standard methods (Longo et al., 2016), plus an additional purification with silver-thiolate functionalized silica gel for samples that featured complex matrices. Briefly, freeze-dried sediments were extracted with dichloromethane:methanol (9:1, v/v) using a Dionex™ accelerated solvent extraction (ASE) system (120 °C and 1200 psi). The extracts were separated into acid and neutral fractions by flash column chromatography with Supelco Supelclean LC-NH_2 (45 μm, 60 Å). Neutral compounds were eluted with dichloromethane/isopropanol (2:1, %v/v), followed by acidic compounds with 4% glacial acetic acid in ethyl ether. The neutral fractions were further separated into alkane, ketone and polar fractions by flash column chromatography using silica gel (40–63 μm, 60 Å) and eluting with hexane, dichloromethane and methanol, respectively. The ketone fraction was saponified, then purified again by elution through a silica gel column with dichloromethane before analysis by GC-MS and GC-FID. When co-eluting compounds were present in the LCA region of a given chromatogram, samples were re-purified by way of silver-thiolate functionalized silica gel (AgTCM; Aponte et al., 2012) using flash column chromatography (Zheng et al., 2017). Saponified ketone fractions purified in this manner were eluted through a 5 cm column of AgTCM with solvents of increasing polarity (hexane:dichloromethane [1:1], dichloromethane, and acetone;). LCAs eluted in the acetone fraction and were re-analyzed by GC-FID and GC-MS. Nine samples required AgTCM purification: G-01, G-02, G-04, G-05, G-12, G-13, G-14, G-16, G-17.

Sediment core or sediment trap samples archived from previous studies were either obtained from the University of Minnesota National Lacustrine Core Facility (LacCore), Minneapolis, Minnesota, USA, or directly from collaborators. Information on archived samples can be found

in references listed in Table S1. Most archived samples were shipped to Brown University as freeze-dried sediments and processed in the same manner as the surface sediments. A portion of the samples underwent initial processing elsewhere, using analogous methods and were shipped to Brown University as lipid extracts. Samples G-06—G-08 and G-18 were processed at Lamont Doherty Earth Observatory, USA; samples G-21—G-24 and G-35 and G-36 were processed at the University of Hong Kong, Hong Kong.

2.1.3. Sediment trap collections

We also analyzed sediments collected in sediment traps from Toolik Lake (2013 and 2014; 68.632 °N, 149.602 °W) and Lake E5 (2014; 68.643 °N, 149.458 °W) to investigate the seasonality of LCA production. Accompanying water column and surface sediment LCA data for these lakes can be found in Longo et al. (2016). Sediment traps were initially deployed during full or partial spring season ice cover and were fixed 2 m above the lake bottom. Sediment traps were collected every 2 to 6 weeks during the ice-free season (June – September) to afford time series of LCA fluxes to the sediment. Sediment trap samples were processed in the same manner as surface sediment samples.

2.2. Analytical methods

All LCAs reported in this study were analyzed with an Agilent 7890B GC system equipped with a flame ionization detector (FID) and an Agilent VF-200ms capillary column (60 m x 250 μm x 0.10 μm). The analytical methods were identical to those used by Longo et al. (2016), which took advantage of improved LCA separation from the mid-polarity GC stationary phase (Longo et al., 2013). Briefly, internal standard (18-pentatricontanone) was added to the purified neutral

fractions, which were dissolved in hexane and introduced to the GC system using pulsed splitless injection (20 psi at 320 °C) and a splitless single-taper liner with glass wool. H_2 was used as the carrier gas and the column flow rate was 36 cm s^{-1}. The following oven program was used: initial temperature of 60 °C (hold 1 min), ramp 20 °C/min to 255 °C, ramp 3 °C/min to 320 °C (hold 10 min). LCA peak identification was accomplished by retention time comparison with a standard containing the 16 LCAs considered in this study and by GC-MS, performed using an Agilent 6890N GC system coupled to an Agilent 5973N quadrupole mass spectrometer. The GC conditions used for GC-MS analysis were the same as those used for GC-FID. The MS was set to an ionization energy of 70 eV and a scan range of 40-600 *m*/*z*. Quantitation of LCAs was accomplished by GC-FID using a single point internal standard method. Analytical precision was determined based on replicate analyses of samples and standards. The following analytical errors for the U^K_{37} index as well as LCA distribution parameters are reported here as ± 1SD (± SE) : U^K_{37}, 0.004 (0.0005); C_{37}/C_{38}, 0.015 (0.002); $\%C_{37:4}$, 0.003 (0.0004); RIK_{37}, 0.002 (0.0003); RIK_{38E}, 0.035 (0.0051).

2.3. Alkenone distribution parameters

Here we focus on four LCA distribution parameters for the purposes of quantitatively comparing and classifying LCA distributions in environmental samples. Traditional distribution parameters include $\%C_{37:4}$ ($\%C_{37:4}$ = 100*([$C_{37:4}$] / [C_{37} LCAs]); Rosell-Melé, 1998) and C_{37}/C_{38} (C_{37}/C_{38} = [C_{37} LCAs] / [C_{38} LCAs]; Volkman et al., 1995). We also considered LCA distribution parameters describing the tri-unsaturated isomeric LCAs, RIK_{37} and RIK_{38E} (Longo et al., 2016),

$$RIK_{37} = \frac{[C_{37:3a}]}{[C_{37:3a} + C_{37:3b}]} \quad (1)$$

$$RIK_{38E} = \frac{[C_{38:3a}Et]}{[C_{38:3a}Et + C_{38:3b}Et]} \quad (2)$$

where the "*a*" and "*b*" subscripts refer to the $\Delta^{7,14,21}$ and $\Delta^{14,21,28}$ tri-unsaturated LCAs, respectively (Longo et al., 2016).

2.4. Alkenone distribution synthesis data

Various datasets from algal culturing studies were compiled to determine species- and/or phylotype-specific LCA distribution parameters for comparison with the Northern Hemispheric freshwater lake dataset. We prioritized studies that i) reported concentration or fractional abundance data for all individual LCAs observed in the samples and ii) varied environmental and biological conditions (primarily growth phase and salinity) in addition to temperature, in order to best capture the full range of variability in LCA distribution parameters. Ranges for *E. huxleyi* distribution parameters were determined from strains B21, G1779Ga, M181, S. Africa and Van556 reported by Conte et al. (1998); strain Van556 reported by Longo et al. (2016); and strain NEP reported by Prahl et al. (1988). *G. oceanica* distribution parameters were determined from strain AB1 reported by Conte et al. (1998) and Strain JB02 reported by Volkman et al. (1995). *I. galbana* distribution parameters were determined from strains CCMP1323 reported by Longo et al. (2016) and strain UTEX LB 2307 reported by Ono et al. (2012). *Ruttnera lamellosa* distribution parameters were determined from strains CCMP1307 reported by Longo et al. (2016) and Nakamura et al. (2014); and strain LX reported by Sun et al. (2007). *Tisochrysis lutea* distribution parameters were determined from strain CCMP463 reported by Longo et al. (2016) and Nakamura et al. (2016); and strain NIES-2590 reported by Nakamura et al. (2016).

Because Group I haptophyte species have never been isolated and grown in culture, we report Group I distribution parameters based on environmental samples from lakes where phylogenetic

analyses (based on 18S ribosomal RNA; Coolen et al., 2004) indicate Group I haptophytes are the LCA-producers. These samples include the *in situ* calibration data from Longo et al. (2016; phylogenetic analysis from Crump et al., 2012); surface sediment from Upper Murray Lake (LCAs analyzed for this study; phylogenetic analysis from Theroux et al., 2010); surface sediment from Lake Toyoni (LCAs analyzed for this study; phylogenetic analysis from McColl et al., 2016); Étang des Vallées (LCAs analyzed for this study; phylogenetic analysis from Simon et al., 2013); and Braya Sø (LCA analysis from Longo et al., 2013; phylogenetic analysis from D'Andrea et al., 2006).

2.5. Climate data and temperature regressions

Climate data for all sites were extracted from the WorldClim Global Climate Database (worldclim.org; Hijmans et al., 2005) using the Senckenberg data extraction tool (dataportal-senckenberg.de/dataExtractTool). WorldClim data are derived from monthly temperature and precipitation data compiled from globally distributed weather stations by the Global Historical Climatology Network, the World Meteorological Organization, the Food and Agriculture Organization of the United Nations, and others. Data are interpolated to 30 arc sec grids and corrected for elevation using NASA Shuttle Radar Topography Mission elevation data and established lapse rates.

Higher resolution climate data for sediment trap time series were downloaded from the Toolik Field Station Environmental Data Center (Environmental Data Center Team, 2017). Air temperatures were measured hourly at 5 m height using a Campbell Scientific HMP155A-L Temperature Probe. Lake temperatures were measured in 3-hourly time steps in Toolik Lake

using a Campbell Scientific 107 Temperature Probe, fixed ~2 m below the lake surface. In the case of Lake E5, lake temperatures taken at 2 m depth were measured periodically throughout the season by the Arctic Long Term Ecological Research program (ARC LTER Database) using a Hach Hydrolab water column sensor array.

For the purposes of temperature regression with the Northern Hemispheric dataset, we explored and used various WorldClim data products including mean monthly temperatures and bioclimatic variables. We focused on mean annual air temperature (MAAT), mean temperature of the spring isothermal season (average temperature of the four months centered on the spring isotherm; MTSI), and mean temperature of the warmest quarter (MTWQ). MTSI represents the spring melt or ice-off season, which has been shown to coincide with high LCA production in freshwater lakes (Longo et al., 2016). In the case of Étang des Vallées, mean monthly temperatures remained above zero all year, and the four months beginning with the coldest month of the year were used for MTSI. Climate zone classifications are according to the Köppen classification system. Water chemistry and lake morphometric data were compiled from published sources referenced in Table S1.

Linear regressions of various temperature metrics *vs.* unsaturation indices were performed on a subset of the freshwater lakes dataset (Table S2) including all surface sediments and all sediment core samples from < 5 cm depth below the lake floor (cmblf). Deeper core samples, core samples with poorly constrained cmblf, and SPM samples were omitted because they are not representative of the decadally-averaged contemporary temperatures from the WorldClim database. We also included 8 representative fresh and oligohaline lacustrine surface sediment

samples with Group I-type distributions (RIK_{37} < 0.63) from northern Alaska and interior Canada (Longo et al., 2016), and 5 oligohaline lacustrine surface sediments from Greenland that have phylogenetically confirmed Group I LCA-producers (D'Andrea et al., 2005).

3. Results and Discussion

3.1 Confirmation of distinct alkenone distributions from Group I haptophytes

New LCA analyses from three lakes that host LCA-producers from the Group I phylotype (confirmed by phylogenetic analysis of 18S ribosomal RNA) support the hypothesis that these organisms produce a specific LCA distribution. Lake Toyoni (G-11), Upper Murray Lake (G-15), and Étang des Vallées (G-04) were previously shown to host Group I haptophytes (Theroux et al., 2010; Simon et al., 2013; Longo et al., 2016; McColl, 2016). Our new LCA analyses revealed that their surface sediments all featured Group I-type LCA distributions, characterized by abundant $C_{37:4}$, the presence of $C_{38:3}$Me LCAs (D'Andrea et al., 2005; 2006), and the full complement of 16 C_{37}-C_{39} LCAs including 4 tri-unsaturated isomers with $\Delta^{14,21,28}$ double bond positioning (Tables 1, S1; Fig. 2b). Previous studies describing Group I-type LCA distributions were restricted to samples collected in Arctic lakes (Longo et al., 2013; 2016; D'Andrea et al., 2016). The addition of samples from lakes in continental and temperate climates (Lake Toyoni and Étang des Vallées) suggest that these LCA distributions are derived from phylotype-specific biosynthetic pathways that are not physiologically restricted to cold environments.

The distinctive LCA distribution shared by Group I haptophytes is intriguing considering that the phylotype, which appears to include the "Greenland Haptophyte" clade (D'Andrea et al., 2006; Theroux et al., 2010) as well as the "EV" clade (Simon et al., 2013), contains considerable genetic diversity. Phylogenetic analyses combining several EV sequences with a Braya Sø water column sequence from Greenland indicate more genetic variation within the Group I phylotype than is observed between Group I and its adjacent Group II phylotype (Longo et al., 2016), which commonly occurs in saline lakes (Coolen et al., 2004; Coolen et al., 2013). This suggests

there are likely subgroups within Group I that may be adapted to different environmental conditions. Currently, however, too few environmental DNA sequences exist to quantitatively test this hypothesis.

Group I LCA distributions are consistent despite genetic variation within the phylotype potentially because the aspects of LCA biosynthesis that differentiated the Group I distribution evolved early in the clade's divergence from its marine ancestors. Later genetic differentiation occurring after freshwater lakes were colonized by Group I, potentially was not associated with changes in LCA biosynthesis and therefore allowed for the Group I distribution to persist even as the Group I haptophytes continued to disperse and evolve. This explanation would be corroborated by the phylogenetic evidence that the divergence of the monophyletic EV clade represents a discrete colonization of freshwater environments by marine haptophytes (Simon et al., 2013). Furthermore, a potential driver of the significant genetic diversity within Group I could be that the organisms are symbionts and therefore have accelerated evolutionary rates (Simon et al., 2013). To determine the true genetic diversity of the Group I phylotype and further test for its effects on LCA distributions, future studies will need to physically describe Group I haptophytes and subject them to controlled culture experiments.

3.2. Alkenone occurrence and distributions in freshwater lakes

Although the pioneering discovery and temperature calibrations for lacustrine LCAs originated from freshwater lakes (Cranwell et al., 1985; Zink et al., 2001), LCAs are rarely reported from freshwater systems potentially because concentrations can be low compared with saline and oligohaline lakes (Chu et al., 2005; D'Andrea et al., 2005; Longo et al., 2016; Plancq et al.,

2018). We found that LCAs were relatively common in freshwater lakes from a range of different climate zones (tundra, subarctic, humid continental and temperate oceanic; mean annual air temperature range: -17.3—10.9 °C; mean annual precipitation range: 125—1657 mm year-1; latitude range: 40—81 °N). Of the 15 freshwater lakes we analyzed that (to our knowledge) had never been investigated for LCAs, 9 of these lakes contained LCAs, which all featured Group I-type distributions (Table 1; Fig 2).

Longo et al. (2016) found that LCA concentrations from freshwater lakes in Alaska were positively correlated with pH, conductivity, alkalinity and mean depth, and efforts were made to sample lakes with similar or higher pH and mean depth values than the LCA-containing northern Alaskan lakes. We focused some of our sampling on volcanic lakes because the mafic bedrock and basin morphometry of these systems may provide optimal ranges for the aforementioned environmental variables. The four volcanic lakes analyzed in this study all contained LCAs (Erlongwan; Ichino-megata; Wudaliangchi; Xianhe; Table S1). Interestingly, we did not detect LCAs in some lakes with elevated pH, and furthermore, geography did not appear to affect LCA occurrence within our sample set. This suggests that additional variables, such as water chemistry, lake morphometry and mixing dynamics likely play roles in determining the occurrence Group I LCAs through their effects on haptophyte ecology (e.g. Toney et al., 2010; Plancq et al., 2018).

Freshwater lakes that had been previously analyzed for LCAs in Germany (G-02, G-05, G-12; Zink et al., 2001), northeast China (G-19; Chu et al., 2005), Hokkaido, Japan (G-11; McColl et al., 2016), and Ellesmere Island, Canada (G-15; Theroux et al., 2010) were originally analyzed

with methods that did not fully separate LCA distributions. Our new analyses demonstrated that these samples all contained the tri-unsaturated isomers and that their distributions were characteristic of Group I-type haptophytes (Table 1; Fig. 2). In total, 20 new analyses from LCA-containing freshwater lakes all produced Group-I type LCA distributions with relatively little variability in the fractional abundances of the 16 LCAs analyzed (Fig. 2a).

To quantitatively assess the similarity between LCA distributions in our Northern Hemispheric freshwater lakes sample set and those of known Group I LCA-producers, we report distribution parameters for the Group I phylotype. Group I distribution parameters were derived from samples with phylogenetically confirmed Group I LCA producers (section 2.4). Mean values and absolute ranges were as follows: C_{37}/C_{38}, 1.16 (range: 0.84-1.54); $\%C_{37:4}$, 53.9 (range: 36.5-65.0); RIK_{37}, 0.56 (range: 0.53-0.60); RIK_{38}, 0.30 (range: 0.17-0.57). While some of these distribution parameters are temperature sensitive, we note that our phylogenetically confirmed Group I samples are derived from sites that experience a broad temperature range (MAAT: -17.3 – 10.4 °C; MTSI: -4.35 – 5.75 °C; MTWQ: 0.9 – 18.9 °C) and therefore should be representative.

Samples from the Northern Hemispheric freshwater lakes (Table 1) and previously published freshwater samples from northern Alaska (Longo et al., 2016) all plotted within or close to the Group I ranges for all of the distribution parameters (Fig. 3). Overall, the freshwater lake samples indicated slightly more variability in LCA distributions than was observed from the phylogenetically confirmed Group I samples. In particular, C_{37}/C_{38}, RIK_{37} and RIK_{38E} all included values that were marginally lower than the Group I range and one SPM sample from

lake Ichino-megata (G-09) gave a C_{37}/C_{38} value significantly greater than the Group I range (Fig. 3). The estimated ranges for these parameters may be too narrow and more samples with phylogenetically confirmed Group I producers may be needed to define the full range of variability in Group I distribution parameters. Nonetheless, the consistency in the LCA distributions (Figs. 2, 3) suggests that LCA production in freshwater lakes is dominated by haptophytes of the Group I phylotype.

3.3 Identifying species effects using alkenone distribution parameters

We examined Group I-type LCA distributions in the context of other species and phylotypes to evaluate methods for differentiating LCA distributions based on the phylogenetic placement of their producers (Fig. 3; Table S3). Traditional distribution parameters ($\%C_{37:4}$ and C_{37}/C_{38}) differentiated the Group I/freshwater LCA distributions from many of the Group II and III species distributions, however there were notable deficiencies. The range of $\%C_{37:4}$ values for *R. lamellosa* (a lacustrine Group II haptophyte) completely overlapped with the Group I range. C_{37}/C_{38} ranges for all Group III species and *R. lamellosa* overlap with the Group I range, rendering C_{37}/C_{38} a poor metric for resolving species or phylotypes. Used in tandem, $\%C_{37:4}$ and C_{37}/C_{38} were unable to fully differentiate Group I-type distributions from *R. lamellosa* distributions of the Group II phylotype (Fig. 3a). This supports the findings of Theroux et al. (2010) that traditional LCA distribution parameters ($\%C_{37:4}$ and C_{37}/C_{38}) are not always sufficient for relating LCA distributions to their parent phylotype.

In contrast, the freshwater lakes dataset confirmed that the tri-unsaturated LCA isomers are robust chemotaxonomic indicators for the Group I phylotype. The RIK_{37} and RIK_{38E} indices

quantify the abundance of the normal $\Delta^{7,14,21}$ tri-unsaturated LCAs relative to their respective $\Delta^{14,21,28}$ isomers. It was proposed that Group I haptophytes produce C_{37} tri-unsaturated isomers in roughly equal abundance with slight preference for the $\Delta^{7,14,21}$ isomer ($C_{37:3a}$). This led to the definition of an RIK_{37} range of 0.51 – 0.60 for the Group I phylotype, based on SPM and surface sediment samples from northern Alaska (Longo et al., 2016). The Group I RIK_{37} distribution parameter reported here from phylogenetically confirmed samples is in strong agreement, with values ranging from 0.53 – 0.60. The entire Northern Hemispheric freshwater lakes dataset also largely agrees with the proposed RIK_{37} range for Group I haptophytes, with values ranging from 0.48 – 0.63 (Table 1; Fig. 3b). Importantly, analyses of several Group II and Group III cultures (Longo et al., 2013; 2016; Theroux et al., 2013; Nakamura et al., 2016; Zheng et al., 2016) have indicated that these phylotypes invariably do not produce the $C_{37:3b}$ isomer, restricting their RIK_{37} values to 1, and fully differentiating them from the Group I/freshwater distributions (Fig. 3b).

The RIK_{38E} index was shown to be sensitive to changes in temperature potentially making it a new LCA-based temperature proxy (Longo et al., 2016). It could offer benefits over U^K indices when LCAs are differentially degraded based on their degree of unsaturation. Rontani et al. (2013) demonstrated that LCA distributions can be significantly augmented from to prolonged oxygen exposure, bacterial degradation, and thiyl radical-induced stereomutation. Therefore, the RIK_{38E} index could be useful for samples from depositional environments where these processes bias U^K_{37} measurements. Here we show that the index can also be used to differentiate LCA distributions by phylotype. RIK_{38E} shows a relatively large range in values for the phylogenetically confirmed Group I samples (0.17-0.57) and a larger range when considering

both Northern Hemispheric and northern Alaskan freshwater samples (0-0.57; Fig. 3b). Although *I. galbana* and *R. lamellosa* were shown to produce $C_{38:3b}$Et LCAs in culture, their abundance relative to $C_{38:3a}$Et is low, resulting in RIK_{38E} values of 0.75-1 (Longo et al., 2016). This allows for the full separation of Group I/freshwater distributions from Group II and III distributions based on RIK_{38E}. Used in tandem or individually, the RIK_{37} and RIK_{38E} indices completely differentiate Group I-type LCA distributions from Group II or Group III distributions, offering improved parameters for identifying species mixing in environmental samples (Fig. 3b).

3.4 Quantifying phylotype mixing using the RIK_{37} index

Distribution parameters suggest that RIK_{37} is most effective in differentiating Group I-type LCA distributions (Fig. 3). Therefore, we employed RIK_{37} in a simple binary mixing model to quantify phylotype mixing in samples with mixed Group I/II distributions. Mixed distributions can occur in oligohaline or brackish environments where the salinity ranges for both phylotypes overlap, or in sediment samples that integrate temporal salinity changes within the lake. This analysis assumes Group I and Group II phylotypes to be the only possible end members because the samples of interest are derived from lakes and therefore should not include Group III marine haptophyte species. The model takes the form,

$$f_{GI}\left(RIK_{37,GI}\right) + f_{GII}\left(RIK_{37,GII}\right) = RIK_{37,sample} \quad (3)$$

$$f_{GI} + f_{GII} = 1 \quad (4)$$

where *f* is the percent contribution of LCAs from Group I or Group II, as defined by the subscripts *GI* and *GII*, respectively. $RIK_{37,GI}$ is the Group I RIK_{37} end member calculated from

our phylogenetically confirmed samples (0.56 ± 0.028*SD*) and $RIK_{37,GII}$ is held at 1.00 since Group II species have never been observed to produce the $C_{37:3b}$ isomer. The error in the Group I end member is propagated through the mixing model after Phillips and Gregg (2001).

We used the model to quantify phylotype mixing in surface sediment samples with clear evidence of mixed Group I/II distributions, including two oligohaline sites in interior Canada (Shannon Lake and Humboldt Lake; Toney et al., 2011; Longo et al., 2016) and sample G-23 from this study, a sediment sample from 32.5 cm depth in core Yarkov-18 from Yarkov Basin, Chany Lake, Siberia (Song, 2016a). Yarkov Basin is currently mesohaline (Table 1), however the mixed distribution at 32.5 cm suggests a fresher lake in the past. For each of the mixed distributions, the model estimates percent contributions from both phylotypes with low error, because of the well-resolved RIK_{37} end members for Group I and Group II distributions (Table 2; Fig. 4).

The RIK_{37} approach to quantifying species mixing is ideal for validating temperature reconstructions from freshwater lakes. Available genetic data indicate that Group I haptophytes occur in fresh to oligohaline conditions, whereas Group II species occupy a wide range of oligohaline to hyperhaline environments (Coolen et al., 2004; 2013; Theroux et al., 2010; Longo et al., 2016). In theory, LCA-based temperature reconstructions from freshwater lakes are unaffected by species effects. However, past periods of elevated salinity recorded in any given sedimentary record, potentially induced species shifts from Group I to Group II haptophytes. Here we demonstrate that RIK_{37} can be used to determine if and when U^{K}_{37} temperature reconstructions are compromised in this manner.

Although species mixing complicates temperature estimates, it can provide valuable information on changes in paleosalinity. LCA distributions have been used to reconstruct salinity and/or effective moisture changes in a number of settings (e.g. Coolen et al., 2004; He et al., 2013; Warden et al., 2016). The mechanisms through which distributions track salinity likely include a minor physiological response in $\%C_{37:4}$ production (Blanz et al., 2005), but are influenced to a much greater extent by salinity-induced shifts in haptophyte species assemblages (e.g. Coolen et al., 2004; 2013; Chivall et al., 2014; Randlett et al., 2014; Longo et al., 2016). Our mixing model results demonstrate that the RIK_{37} index can be employed to reconstruct paleosalinity changes with mixed Group I/II LCA distributions indicating oligohaline conditions in which both Group I and II haptophytes thrive. Group I-type distributions (RIK_{37} = 0.48 – 0.63) indicate a fresh to oligohaline salinity range and Group II-type distributions (RIK_{37} = 1) indicate oligohaline to hypersaline environments (Longo et al., 2016). In time series, secular increases (decreases) in RIK_{37} between 0.63 and 1 can be interpreted to indicate increasing (decreasing) lake salinity. Thus, the RIK_{37} index has applications for both paleotemperature and paleosalinity reconstructions.

3.5 Alkenone temperature response and production seasonality in freshwater lakes

Evidence demonstrating coherent U^K_{37} temperature sensitivities among Group I haptophytes upholds the possibility that a global Group I temperature calibration could be developed. Three *In situ* temperature calibrations from lakes with phylogenetically confirmed Group I haptophyte producers (D'Andrea et al., 2011; 2016; Longo et al., 2016) demonstrate linear responses of U^K_{37} to temperature, with calibration slopes ranging from 0.021 to 0.030. Another surface sediment

calibration from German freshwater lakes also falls within this range (0.0211; Zink et al., 2001) and our analyses indicate that lakes used in the calibration (G-02; G-05; G-12) contain Group I-type distributions. The range in slopes among these four Group I temperature calibrations is narrow compared with the variability in calibration slopes between phylotypes (D'Andrea et al., 2016; Longo et al., 2016). Therefore, we examined relationships between LCA unsaturation and temperature to assess whether a global Group I temperature calibration might be feasible.

The seasonality of LCA production has the potential to significantly affect various temperature calibration statistics; therefore we carried out sediment trap experiments from two dimictic freshwater lakes in northern Alaska to first determine the seasonality of sedimentary fluxes of LCAs. Toolik Lake and Lake E5 show the highest sedimentary fluxes of LCAs during the spring transitional season (Fig. 5; Table S4). In each of three time series (Toolik Lake 2013; 2014; Lake E5 2014) LCA fluxes peaked in the first sediment trap collection, indicating that LCA production occurred during the period of partial ice cover, isothermal mixing and incipient stratification. The LCA fluxes were attenuated or reached zero before the lakes reached their maximum temperature and U^{K}_{37} inferred temperatures of the sediment trap LCAs were consistent with lake temperatures during ice melt and isothermal mixing (Table S4; Longo et al., 2016). Notably, there were significant lake-to-lake and year-to-year differences in the magnitude of LCA fluxes, however the seasonality of the flux was consistent among all time series (Fig. 5).

While these findings only represent one geographic location, additional studies focusing on Group I haptophytes from lakes in Norway and Greenland have demonstrated high sedimentary fluxes of LCAs during the spring transitional season (D'Andrea et al., 2011; D'Andrea et al.,

2016). Alkenones from Group II haptophytes in Lake George, in the continental United States also indicate high water column concentrations of LCAs during the spring, which decrease significantly with the onset of thermal stratification (Toney et al., 2010). Together, these studies along with our new data from northern Alaskan lakes suggest that lacustrine LCA-producing haptophytes bloom and produce LCAs during the spring.

In addition to seasonality, the depth habitats of LCA-producing haptophytes also have the potential to greatly affect temperature calibrations. While some members of the Group II phylotype are benthic species (Rontani et al., 2004), recent work suggests that Group I haptophytes bloom and produce LCAs in the photic zone of the water column. For example, Theroux et al., (2012) observed concurrent maxima in LCA concentrations and Group I haptophyte rRNA gene copies in the metalimnion of Lake Braya Sø, Greenland. Additional studies have demonstrated high concentrations of LCAs with Group I-type distributions in the epilimnion and metalimnion of lakes in Alaska and Greenland, with their U^{K}_{37} values responding to short-term water temperature fluctuations, indicative of in situ water column production (D'Andrea et al., 2011; Longo et al., 2016). Consequently, these data including Group I haptophyte DNA and biomarker analyses demonstrate that Group I LCAs record the lake temperature of the photic zone during the spring transitional season, which is sensitive to lake ice accumulation in the winter and the rate of lake ice melt and lake warming in the spring.

With the seasonality and depth habitat of Group I haptophytes accounted for, we used the Northern Hemispheric dataset to investigate the large-scale response of LCA unsaturation to temperature (Fig. 6). U^{K}_{37} values generally increased with decreasing latitude, indicating that C_{37}

LCAs produced at warmer sites were more saturated than those produced in colder environments (Fig. 6a). MAAT, MTSI and MTWQ were all significantly positively correlated with U^K_{37}. MAAT was weakly correlated with U^K_{37} ($U^K_{37} = 0.0075*T - 0.49$; $r^2 = 0.35$; $p = 0.0028$; Fig. 6b) compared with the season-specific temperature metrics MTSI ($U^K_{37} = 0.029*T - 0.49$; $r^2 = 0.60$; $p < 0.0001$; Fig. 6c) and MTWQ ($U^K_{37} = 0.013*T - 0.66$; $r^2 = 0.52$; $p < 0.001$; not shown). The strongest correlation of U^K_{37} with MTSI is consistent with our observations of high sedimentary fluxes of lacustrine LCAs occurring in the spring transitional season.

In addition to showing the strongest correlation, the regression of U^K_{37} with MTSI also produces a slope (0.029) that is within the range in slopes shown by the four known Group I calibrations (0.021 – 0.030; Zink et al., 2001; D'Andrea et al., 2011; 2016; Longo et al., 2016), whereas the MTWQ and MAAT regressions both result in slopes well below this range. We applied the three calibrations available from freshwater lakes with evidence of Group I LCA-producers (Zink et al., 2001; D'Andrea et al., 2016; Longo et al., 2016) to reconstruct lake temperatures for the Northern Hemispheric freshwater lakes dataset, and grouped the lakes by their climate zones (Fig. 5e-5f). Predicted lake temperatures differ somewhat among the calibrations, however all predicted temperatures fell within a reasonable range (-1 – 20 °C) and the prevalence of predicted temperatures below 15 °C for mid-latitude sites and below 8 °C for Arctic tundra sites is consistent with our interpretation that U^K_{37} records spring lake temperature.

While the correlation of U^K_{37} with MTSI is strong and statistically significant, only 60% of the variability in U^K_{37} is explained by temperature, indicating that a predictive global freshwater

temperature calibration using surface sediments may not be appropriate. Many factors complicate a global calibration including variability in water chemistry, lake depth and morphometry (which introduce site differences in lake temperature sensitivity to air temperature; Livingstone et al., 1999), and sedimentation rates (which affect duration represented in our surface sediments). Furthermore, some variability among the intercepts of *in situ* Group I calibrations has been documented (D'Andrea et al., 2016; Longo et al., 2016) and while there is not currently an explanation for this phenomenon, it likely adds noise to our regressions. Regardless of these confounding variables, the samples demonstrate the large-scale response of LCA unsaturation to temperature in Group I freshwater lakes.

3.6 Alkenone-based temperature reconstruction in lakes with mixed distributions

The Northern Hemispheric freshwater lakes dataset suggests that mixed LCA distributions should be rare or absent in freshwater lakes; however, phylotype mixing is likely prevalent in oligohaline lakes or lakes with temporally varying salinity (e.g. glacial or snow-melt fed lakes in arid regions). Lakes with mixed LCA distributions highlight the need to develop new temperature proxies that are resilient to mixed LCA distributions. The $C_{37:3b}$ and $C_{38:3b}$Et LCAs present a potential solution to this problem since these compounds are either exclusively ($C_{37:3b}$) or predominantly ($C_{38:3b}$Et) produced by Group I haptophytes in high abundance and therefore likely reflect the temperature response of the Group I phylotype, even in mixed LCA distributions.

LCA distributions derived from SPM samples in Toolik Lake, Alaska indicated that the fractional abundance of the $C_{37:3b}$ isomer was significantly positively correlated with *in situ* lake temperature, whereas the $C_{38:3b}$Et isomer was relatively invariant across a large temperature range (Longo et al., 2016). Therefore the following LCA ratio, R3b,

$$R3b = \frac{[C_{37:3b}]}{[C_{38:3b}Et + C_{37:3b}]} \quad (5)$$

should covary with temperature as $C_{37:3b}$ is preferentially produced at warmer water temperatures. In the Toolik lake *in situ* calibration dataset (Longo et al., 2016), the correlation is highly significant (R3b = 0.0081*T + 0.44; $r^2 = 0.67$; $p << 0.01$; Fig. 7a). Removing the two outliers with the lowest R3b values improves the relationship (R3b = 0.0078*T + 0.45; $r^2 = 0.76$; $p << 0.01$). The Northern Hemispheric lakes dataset also demonstrates a significant yet weak positive correlation between R3b and MTSI (R3b = 0.032*T + 0.42; $r^2 = 0.39$; $p < 0.01$; Fig. 7b).

There is significant variability in the linear regression that may arise from several factors including those previously discussed (section 3.5).

600

U^{K}_{38Me} is a temperature proxy based on the unsaturation of C_{38}Me LCAs (Conte et al., 1993) that could be utilized when mixed Group I/II LCA distributions occur, because Group II species do not appear to produce C_{38}Me LCAs (Conte et al., 1994; Coolen et al., 2004; Rontani et al., 2004; Sun et al., 2007). We consider the following form of U^{K}_{38Me}, which includes the $C_{38:4}$Me and

605 $C_{38:3b}$Me LCAs:

$$U^{K}_{38Me} = \frac{[C_{38:2}Me - C_{38:4}Me]}{[C_{38:2}Me + C_{38:3a}Me + C_{38:3b}Me + C_{38:4}Me]} \quad (6)$$

The *in situ* U^{K}_{38Me} calibration from Toolik Lake (U^{K}_{38Me} = 0.017*T – 0.35; r^2 = 0.77; p << 0.01; Fig. 7c) is robust. While there is also a significant relationship between U^{K}_{38Me} and temperature in the Northern Hemispheric lakes dataset, the correlation is weak (U^{K}_{38Me} = 0.023*T – 0.16; r^2 =

610 0.33; p = 0.016; Fig. 7d) and greatly improves when the two outliers (G-03, INI-004) are removed (U^{K}_{38Me} = 0.030*T – 0.19; r^2 = 0.71; p << 0.01) indicating that environmental variables in addition to temperature may affect U^{K}_{38Me} at larger spatial scales. For both U^{K}_{38Me} and R3b, more studies are needed to determine whether these indices could be viable alternatives to U^{K}_{37} for samples with mixed LCA distributions.

615

4. Conclusions

In this study we analyzed a compilation of samples from freshwater lakes throughout the Northern Hemisphere to address the hypothesis that LCAs in these systems share a distribution derived from one specific phylotype of Isochyrsidales haptophyte algae – the Group I phylotype. Our results provided support for this hypothesis, suggesting that freshwater lakes are generally immune to species effects, which have hindered LCA-based temperature reconstructions in saline lakes and coastal waters. Our analyses show that the RIK_{37} and RIK_{38E} indices can be used to quantitatively differentiate LCAs produced by Group I haptophytes from those produced by other phylotypes, deeming them extremely useful for validating LCA-based temperature reconstructions and for reconstructing salinity-induced shifts in species assemblages. We show for the first time that when species effects are ruled out using the RIK_{37} index, the cross-continental response of LCA unsaturation to temperature is significant and observable in lakes. Furthermore, we introduce the R3b index as a potential new temperature proxy to be utilized when mixed Group I/II distributions are present.

The widespread occurrence of Group I-type LCA distributions provides evidence that Group I haptophytes are not specific to Arctic environments. Therefore, caution should be taken when analyzing LCAs from any environment (lake, estuary or coastal sea), which may have been subjected to periods of low salinity (fresh to mesohaline). Analysis of such samples with methods that do not fully separate the tri-unsaturated isomers, can result in the loss of valuable paleoecological and paleoclimatic information. As we have shown here, the quantification of tri-unsaturated isomers in these samples is prerequisite for determining whether species effects have compromised temperature reconstructions from these environments.

Future studies should aim to further describe the Group I phylotype and isolate its species in pure culture. Even with their consistent LCA distributions, Group I haptophyte species contain considerable genetic diversity and phylogenetic analyses have yet to determine whether the Group I phylotype includes subgroups. More proxy development studies from mid-latitude sites will allow for a better understanding of the seasonality of and environmental controls on LCA production and their effects on temperature reconstruction. Nonetheless, our Northern Hemispheric freshwater lakes dataset has provided a foundation for detecting and controlling for species-effects and interpreting U_{37}^{K} as a spring lake temperature proxy. Because the majority of mid- and high latitude continental temperature proxies represent summer temperatures, the development of a new spring lake temperature proxy sets the foundation for seasonally resolved temperature reconstructions.

Acknowledgements

This work was primarily funded by NSF grant PLR-1503846 to Y. Huang, NSF grant DEB-1026843 to G. Shaver, and the National Geographic Society. We would like to thank A. Carter and D. White for assistance in the field, L. Wang and J. Dillon for discussions on alkenone separations methods, and R. Tarozo who provided laboratory support. Icelandic lake samples were provided by LacCore (National Lacustrine Core Facility), Department of Earth Sciences, University of Minnesota-Twin Cities. We thank R. Bradley for providing the Upper Murray Lake sample. The ARC LTER and Toolik Field Station Environmental Data Center provided air and lake temperature data. Six samples and environmental data from lakes in south Siberia and north Mongolia were supported by RSF, grant 17-77-10086, RFBR and Government of the Novosibirsk Region, grant 17-45-540527, and the Ministry of Education and Science of the Russian Federation (project no. 14.Y26.31.0018). Two samples from Lake Ichino-megata were collected with funding from MEXT-Japan KAKENHI grant nos. 24651019, 2621101002 and 101002. Two samples from volcanic lakes in NE China were collected with funding from the National Natural Science Foundation of China (grant no. 41573113) to Y. Huang. We thank two anonymous reviewers for suggestions that greatly improved the manuscript.

References

Aponte, J.C., Dillon, J.T., Tarozo, R., Huang, Y., 2012. Separation of unsaturated organic compounds using silver-thiolate chromatographic material. J. Chromatogr. A 1240, 83–89.

ARC LTER Database. Available from http://arc-lter.ecosystems.mbl.edu/lakes/lakes-physical-and-chemical-parameters. Accessed April 12, 2016.

Bendif, E.M., Probert, I., Schroeder, D.C., de Vargas, C., 2013. On the description of Tisochrysis lutea gen. nov. sp. nov. and Isochrysis nuda sp. nov. in the Isochrysidales, and the transfer of Dicrateria to the Prymnesiales (Haptophyta). J. Appl. Phycol. 25, 1763–1776.

Blanz, T., Emeis, K.-C., Siegel, H., 2005. Controls on alkenone unsaturation ratios along the salinity gradient between the open ocean and the Baltic Sea. Geochim. Cosmochim. Acta 69, 3589–3600.

Brassell, S.C., Eglinton, G., Marlowe, I.T., Pflaumann, U., Sarnthein, M., 1986. Molecular stratigraphy: a new tool for climatic assessment. Nature 320, 129–133.

Chivall, D., M'Boule, D., Sinke-Schoen, D., Sinninghe Damsté, J.S., Schouten, S., van der Meer, M.T.J., 2014. Impact of salinity and growth phase on alkenone distributions in coastal haptophytes. Org. Geochem. 67, 31–34.

Chu, G., Sun, Q., Li, S., Zheng, M., Jia, X., Lu, C., Liu, J., Liu, T., 2005. Long-chain alkenone distributions and temperature dependence in lacustrine surface sediments from China. Geochim. Cosmochim. Acta 69, 4985–5003.

Conte M. H. and Eglinton G., 1993. Alkenone and alkenoate distributions within the euphotic zone of the eastern North Atlantic: Correlation with production temperature. Deep-Sea Res. Part I 40, 1935–1961.

Conte, M.H., Sicre, M.-A., Rühlemann, C., Weber, J.C., Schulte, S., Schulz-Bull, D., Blanz, T., 2006. Global temperature calibration of the alkenone unsaturation index (UK′37) in surface waters and comparison with surface sediments. Geochemistry, Geophys. Geosystems 7, 10.1029/2005GC001054.

Conte, M.H., Thompson, A., Lesley, D., Harris, R.P., 1998. Genetic and Physiological Influences on the Alkenone/Alkenoate Versus Growth Temperature Relationship in Emiliania huxleyi and Gephyrocapsa oceanica. Geochim. Cosmochim. Acta 62, 51–68.

Conte, M.H., Volkman, J.K., Eglinton, G., 1994. Lipid biomarkers in Haptophyta, In: Green, 655 J.C., Leadbeater, B.S.C. (Eds.), The Haptophyte Algae. Systematics Association Special. 656 Clarendon Press.

Coolen, M.J.L., Muyzer, G., Rijpstra, W.I.C., Schouten, S., Volkman, J.K., Sinninghe Damsté, J.S., 2004. Combined DNA and lipid analyses of sediments reveal changes in Holocene

haptophyte and diatom populations in an Antarctic lake. Earth Planet. Sci. Lett. 223, 225–239.

Cranwell, P.A., 1985. Long-chain unsaturated ketones in recent lacustrine sediments. Geochim. Cosmochim. Acta 49, 1545–1551.

Crump, B.C., Amaral-Zettler, L. a, Kling, G.W., 2012. Microbial diversity in arctic freshwaters is structured by inoculation of microbes from soils. ISME J. 6, 1629–39.

D'Andrea, W.J., Huang, Y., 2005. Long chain alkenones in Greenland lake sediments: Low δ13C values and exceptional abundance. Org. Geochem. 36, 1234–1241.

D'Andrea, W.J., Huang, Y., Fritz, S.C., Anderson, N.J., 2011. Abrupt Holocene climate change as an important factor for human migration in West Greenland. Proc. Natl. Acad. Sci. U. S. A. 108, 9765–9.

D'Andrea, W.J., Lage, M., Martiny, J.B.H., Laatsch, A.D., Amaral-Zettler, L. a., Sogin, M.L., Huang, Y., 2006. Alkenone producers inferred from well-preserved 18S rDNA in Greenland lake sediments. J. Geophys. Res. 111, G03013.

D'Andrea, W.J., Theroux, S., Bradley, R.S., Huang, X., 2016. Does phylogeny control UK37-temperature sensitivity? Implications for lacustrine alkenone paleothermometry. Geochim. Cosmochim. Acta 175, 168–180.

Dillon, J.T., Longo, W.M., Zhang, Y., Torozo, R., Huang, Y., 2016. Identification of double bond positions in isomeric alkenones from a lacustrine haptophyte. Rapid Commun. Mass Spectrom. 30, 112–118.

Environmental Data Center Team., 2017. Meteorological monitoring program at Toolik, Alaska. Toolik Field Station, Institute of Arctic Biology, University of Alaska Fairbanks, Fairbanks, AK 99775.

Harada, N., Shin, K.-H., Murata, A., Uchida, M., Nakatani, T., 2003. Characteristics of alkenones synthesized by a bloom of Emiliania huxleyi in the Bering Sea. Geochim. Cosmochim. Acta 67, 1507–1519.

He, Y., Zhao, C., Wang, Z., Wang, H., Song, M., Liu, W., Liu, Z., 2013. Late Holocene coupled moisture and temperature changes on the northern Tibetan Plateau. Quat. Sci. Rev. 80, 47–57.

Hijmans, R. J., Cameron, S. E., Parra, J. L., Jones, P. G. and Jarvis, A., 2005. Very high resolution interpolated climate surfaces for global land areas. Int. J. Climatol. 25, 1965–1978.

Livingstone, David M., André F. Lotter, and Ian R. Walker., 1999. The decrease in summer surface water temperature with altitude in Swiss Alpine lakes: a comparison with air

temperature lapse rates. Arct. Antarct. Alp. Res., 341-352.

Longo, W.M., Dillon, J.T., Tarozo, R., Salacup, J.M., Huang, Y., 2013. Unprecedented separation of long chain alkenones from gas chromatography with a poly(trifluoropropylmethylsiloxane) stationary phase. Org. Geochem. 65, 94–102.

Longo, W.M., Theroux, S., Giblin, A.E., Zheng, Y., James, T., Huang, Y., 2016. Temperature calibration and phylogenetically distinct distributions for freshwater alkenones: Evidence from northern Alaskan lakes. Geochim. Cosmochim. Acta 180, 177–196.

McColl, J.L., 2016. Climate variability of the last 1000 years in the NW Pacific: high resolution, multi-biomarker records from Lake Toyoni (Doctoral dissertation, University of Glasgow).

Müller, P.J., Kirst, G., Ruhland, G., Von Storch, I., Rosell-Melé, A., 1998. Calibration of the alkenone paleotemperature index UK'37 based on core-tops from the eastern South Atlantic and the global ocean (60°N-60°S). Geochim. Cosmochim. Acta 62, 1757–1772.

Nakamura, H., Sawada, K., Araie, H., Shiratori, T., Ishida, K., Suzuki, I., Shiraiwa, Y., 2016. Composition of long chain alkenones and alkenoates as a function of growth temperature in marine haptophyte Tisochrysis lutea. Org. Geochem. 99, 78–89.

Nakamura, H., Sawada, K., Araie, H., Suzuki, I., Shiraiwa, Y., 2014. Long chain alkenes, alkenones and alkenoates produced by the haptophyte alga Chrysotila lamellosa CCMP1307 isolated from a salt marsh. Org. Geochem. 66, 90–97.

Ono, M., Sawada, K., Shiraiwa, Y., Kubota, M., 2012. Changes in alkenone and alkenoate distributions during acclimatization to salinity change in Isochrysis galbana: Implication for alkenone-based paleosalinity and paleothermometry. Geochem. J. 46, 235–247.

Phillips, D.L., Gregg, J.W., 2001. Uncertainty in source partitioning using stable isotopes. Oecologia 127, 171–179.

Plancq, J., Cavazzin, B., Juggins, S., Haig, H. A., Leavitt, P. R., Toney, J. L., 2018. Assessing environmental controls on the distribution of long-chain alkenones in the Canadian Prairies. Org. Geochem. 117, 43-55.

Prahl, F.G., Muehlhausen, L.A., Zahnle, D.L., 1988. Further evaluation of long-chain alkenones as indicators of paleoceanographic conditions. Geochim. Cosmochim. Acta 52, 2303–2310.

Prahl, F.G., Wakeham, S.G., 1987. Calibration of unsaturation patterns in long-chain ketone compositions for palaeotemperature assessment. Nature 330, 367–369.

Randlett, M.-È., Coolen, M.J.L., Stockhecke, M., Pickarski, N., Litt, T., Balkema, C., Kwiecien, O., Tomonaga, Y., Wehrli, B., Schubert, C.J., 2014. Alkenone distribution in Lake Van sediment over the last 270 ka: influence of temperature and haptophyte species composition. Quat. Sci. Rev. 104, 53-62.

Rontani, J.-F., Beker, B., Volkman, J.K., 2004. Long-chain alkenones and related compounds 734 in the benthic haptophyte Chrysotila lamellosa Anand HAP 17. Phytochemistry 65, 117-126.

Rontani, J.-F., Volkman, J.K., Prahl, F.G., Wakeham, S.G., 2013. Biotic and abiotic degradation of alkenones and implications for U37K′ paleoproxy applications: A review. Org. Geochem. 59, 95–113.

Rosell-Melé, A., 1998. Interhemispheric appraisal of the value of alkenone indices as temperature and salinity proxies in high-latitude locations. Paleoceanography 13, 694–703.

Simon, M., López-García, P., Moreira, D., Jardillier, L., 2013. New haptophyte lineages and multiple independent colonizations of freshwater ecosystems. Environ. Microbiol. Rep. 5, 322–32.

Song, M., 2016a. Hydrological changes in Asian inland since late Pleistocene and climatic implications of interactions between westerlies and East Asian summer monsoon. HKU Theses Online (HKUTO).

Song, M., Zhou, A., He, Y., Zhao, C., Wu, J., Zhao, Y., Liu, W., Liu, Z., 2016b. Environmental controls on long-chain alkenone occurrence and compositional patterns in lacustrine sediments, northwestern China. Org. Geochem. 91, 43–53

Sun, Q., Chu, G., Liu, G., Li, S., Wang, X., 2007. Calibration of alkenone unsaturation index with growth temperature for a lacustrine species, Chrysotila lamellosa (Haptophyceae). Org. Geochem. 38, 1226–1234.

Theroux, S., D'Andrea, W.J., Toney, J., Amaral-Zettler, L., Huang, Y., 2010. Phylogenetic diversity and evolutionary relatedness of alkenone-producing haptophyte algae in lakes: Implications for continental paleotemperature reconstructions. Earth Planet. Sci. Lett. 300, 311-320.

Theroux, S., Toney, J., Amaral-Zettler, L., Huang, Y., 2013. Production and temperature sensitivity of long chain alkenones in the cultured haptophyte Pseudoisochrysis paradoxa. Org. Geochem. 62, 68–73.

Toney, J.L., Huang, Y., Fritz, S.C., Baker, P.A., Grimm, E., Nyren, P., 2010. Climatic and environmental controls on the occurrence and distributions of long chain alkenones in lakes of the interior United States. Geochim. Cosmochim. Acta 74, 1563–1578.

Toney, J.L., Leavitt, P.R., Huang, Y., 2011. Alkenones are common in prairie lakes of interior Canada. Org. Geochem. 42, 707–712.

Volkman, J.K., Barrerr, S.M., Blackburn, S.I., Sikes, E.L., 1995. Alkenones in Gephyrocapsa oceanica: Implications for studies of paleoclimate. Geochim. Cosmochim. Acta 59, 513–

520.

Volkman, J.K., Eglinton, G., Corner, E.D.S., Forsberg, T.E.V., 1980. Long-chain alkenes and alkenones in the marine coccolithophorid Emiliania huxleyi. Phytochemistry 19, 2619–2622.

Wang, Z., Liu, Z., Zhang, F., Fu, M., An, Z., 2015. A new approach for reconstructing Holocene temperatures from a multi-species long chain alkenone record from Lake Qinghai on the northeastern Tibetan Plateau. Org. Geochem. 88, 50-58.

Warden, L., van der Meer, M.T.J., Moros, M., Sinninghe Damsté, J.S., 2016. Sedimentary alkenone distributions reflect salinity changes in the Baltic Sea over the Holocene. Org. Geochem. 102, 30–44.

Zheng, Y., Huang, Y., Andersen, R.A., Amaral-Zettler, L.A., 2016. Excluding the di-unsaturated alkenone in the UK37 index strengthens temperature correlation for the common lacustrine and brackish-water haptophytes. Geochim. Cosmochim. Acta 175, 36–46.

Zheng, Y., Tarozo, R., Huang, Y., 2017. Optimizing chromatographic resolution for simultaneous quantification of long chain alkenones, alkenoates and their double bond positional isomers. Org. Geochem. 111, 136–143.

Zink, K.G., Leythaeuser, D., Melkonian, M., Schwark, L., 2001. Temperature dependency of long-chain alkenone distributions in Recent to fossil limnic sediments and in lake waters. Geochim. Cosmochim. Acta 65, 253–265.

Figures

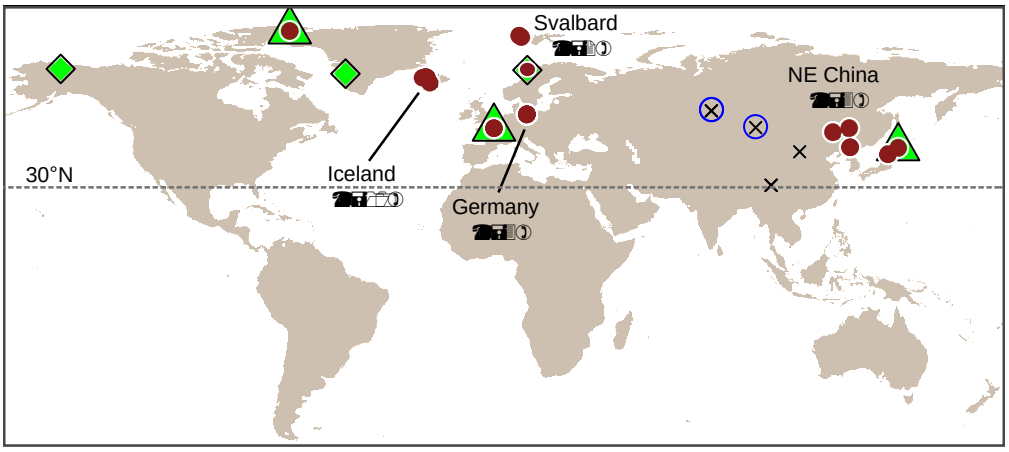

Fig. 1. Map showing the location of all LCA-containing samples analyzed in this study. Samples from freshwater lakes are marked with filled red circles; samples from saline lakes are marked with unfilled blue circles; samples from freshwater lakes with phylogenetically confirmed Group I LCA producers are marked with green triangles. Samples from previous studies with phylogenetically confirmed Group I haptophytes and Group I-type LCA distributions are marked with green diamonds (D'Andrea et al., 2006; 2016; Longo et al., 2013; 2016). Lakes analyzed that did not contain LCAs are marked with an "x." The 30 °N parallel is shown to illustrate the northern mid- and high latitude spatial extent of the dataset.

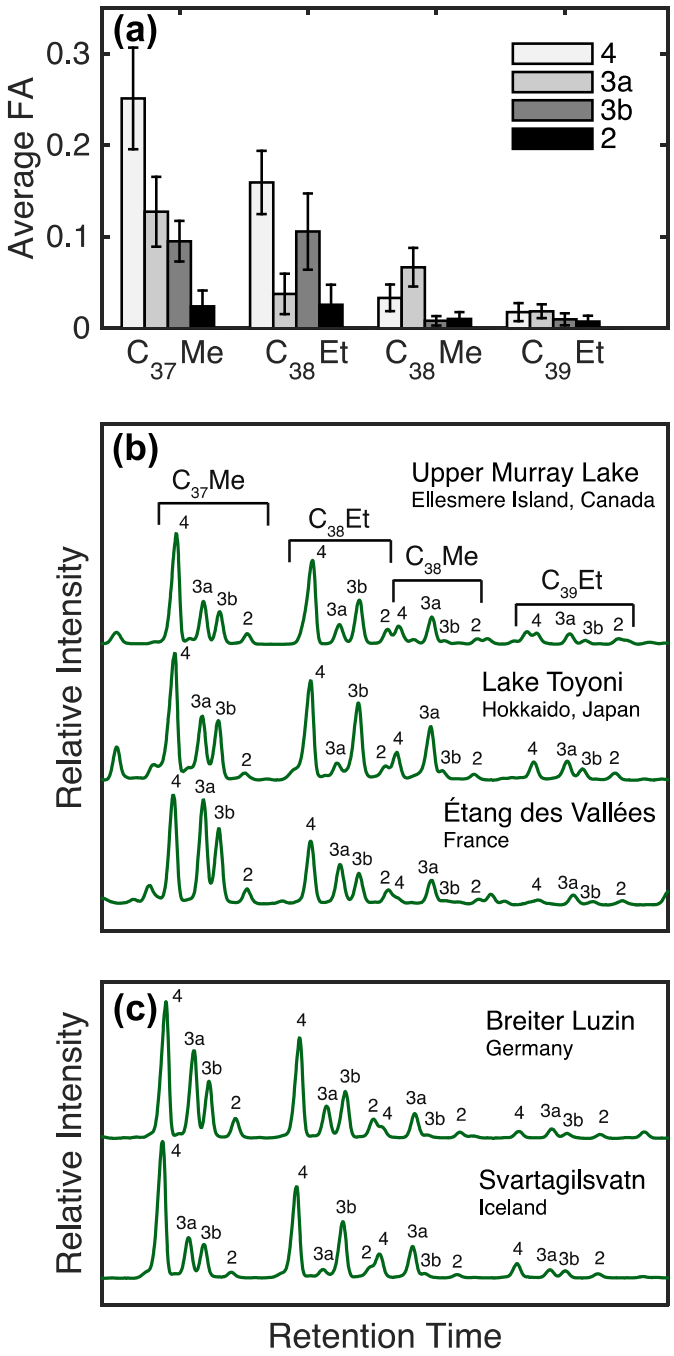

Fig. 2. (a) Mean fractional abundance of LCAs in all freshwater lake samples analyzed in this study (Table 1). Error bars represent ± 1SD. Also shown are partial gas chromatograms of LCAs in (b) surface sediments with phylogenetically confirmed Group I haptophyte producers and (c) sediments from German (Zink et al., 2001) and Icelandic freshwater lakes.

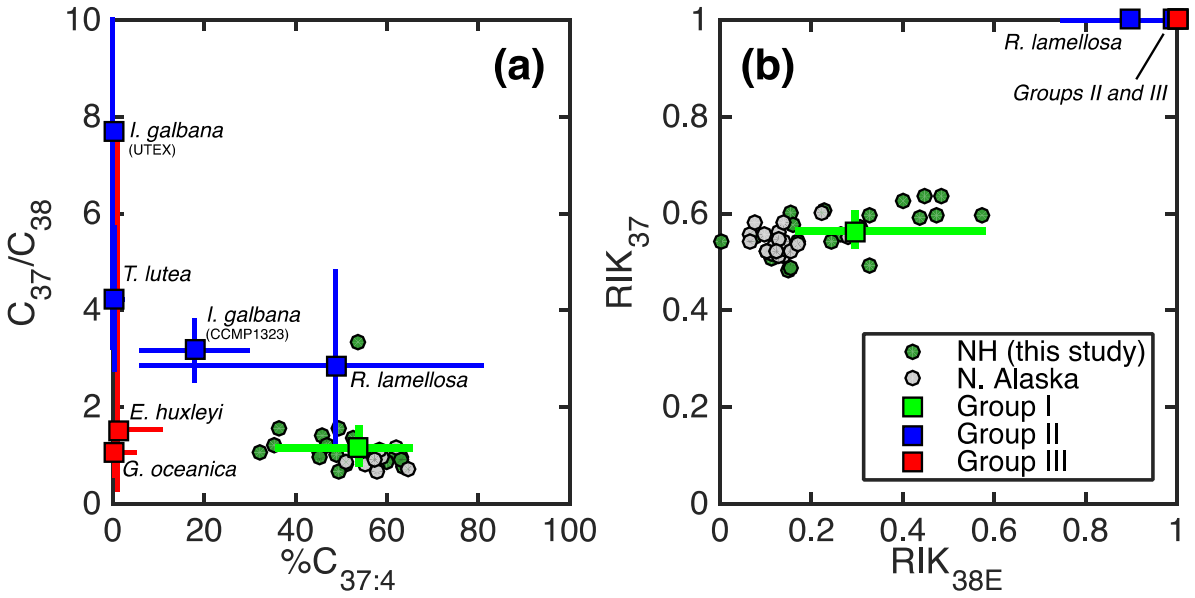

Fig. 3. LCA distribution parameters for surface sediments from the Northern Hemispheric and northern Alaskan (Longo et al., 2016) freshwater lakes datasets. LCA distribution parameters are also plotted by haptophyte species and phylotype based on our synthesis of published culture data (section 2.4). Error bars represent the ranges in distribution parameters and square points represent mean values. (a) Traditional distribution parameters ($\%C_{37:4}$ and C_{37}/C_{38}) are insufficient for differentiating *R. lamellosa* distributions from the Group I phylotype. (b) The RIK_{37} and RIK_{38E} indices fully differentiate all species and phylotypes from the Group I phylotype.

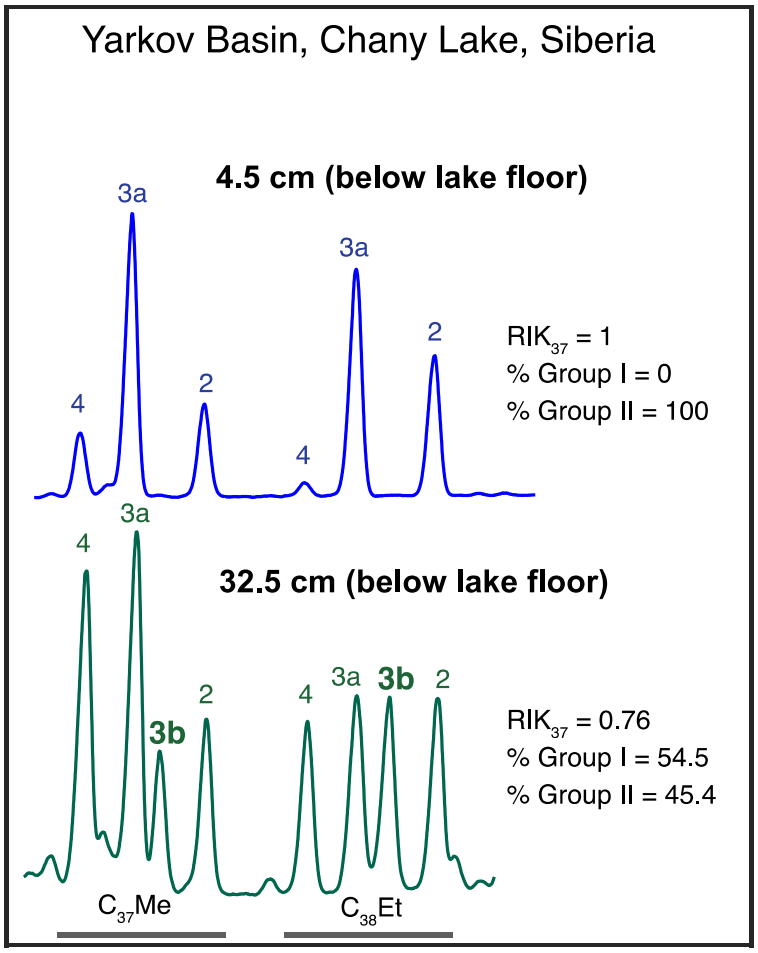

915 **Fig. 4.** Partial gas chromatograms of LCAs from two depths in core Yarkov-18, Yarkov Basin, Chany Lake, Siberia. The modern lake is mesohaline and the recent (4.5 cmblf) LCA distribution reflects a Group II LCA producer. At 32.5 cm depth in the core, a mixed Group I/II LCA distribution is indicated by the presence of $C_{37:3b}$. % contributions of Group I and II LCAs to each sample are determined from the binary mixing model and
920 used to infer changes in salinity between the samples.

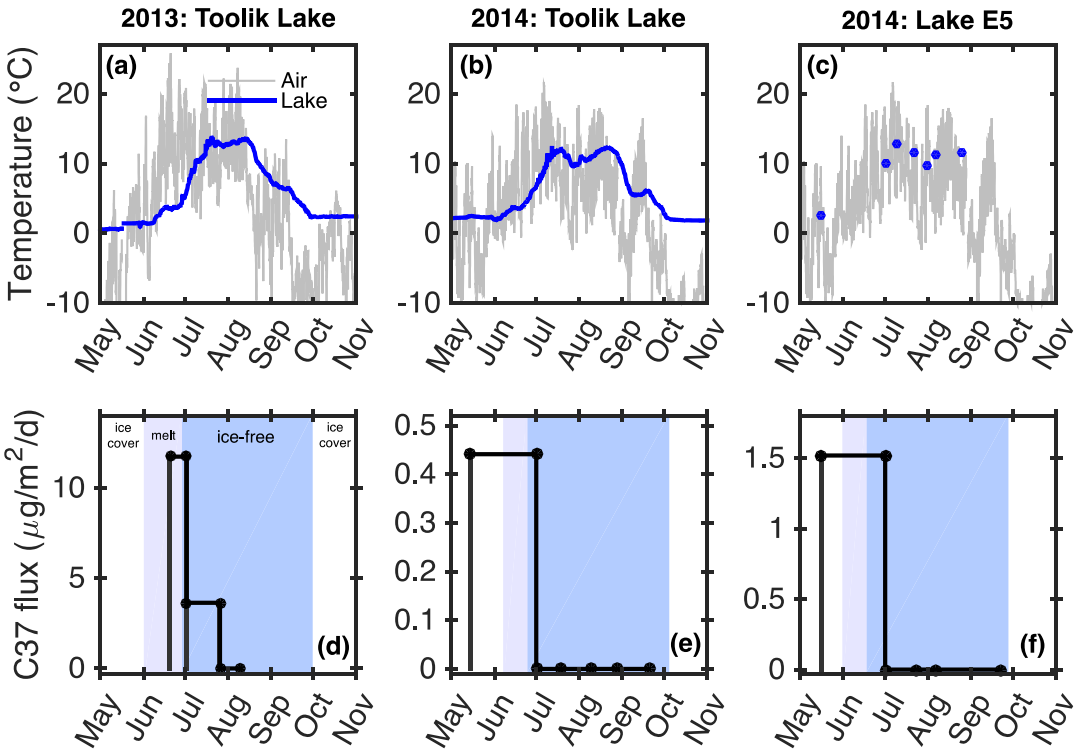

Fig. 5. Sedimentary C_{37} LCA fluxes recorded in sediment traps deployed in two northern Alaskan lakes (d-f) plotted along with lake and air temperature data (a-c). Sediment fluxes were calculated for discrete sediment trap deployment periods, which lasted from 2 to 6 weeks and are delineated by the filled black circles. Shading (in d-f) represents periods of full lake ice cover (white), partial lake ice cover (light blue), and the summer ice-free period (blue).

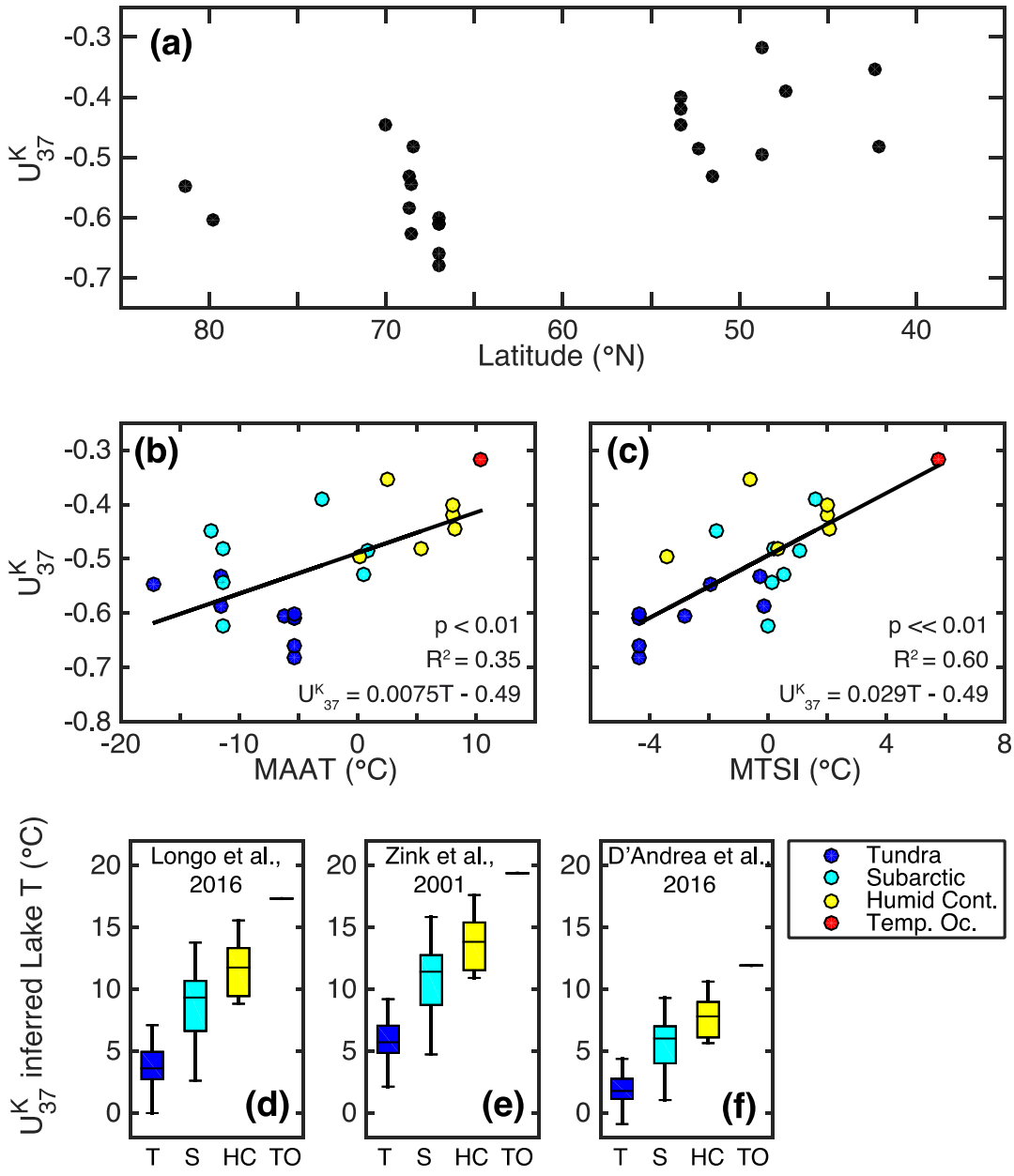

Fig. 6. (a) U^K_{37} vs. latitude for surface sediments from the Northern Hemispheric freshwater lakes dataset (this study), including representative samples from Greenland, Interior Canada and northern Alaska (D'Andrea et al., 2005; Toney et al., 2011; Longo et al., 2016). Unsaturation of C_{37} LCAs increases with decreasing latitude reflecting the large-scale response of Group I LCAs to temperature. U^K_{37} is significantly positively correlated with MAAT (b) and MTSI (c). U^K_{37} inferred lake temperatures range from -1 to 20 °C based on Group I freshwater lake calibrations (d, Longo et al., 2016; e, Zink et al., 2001; f, D'Andrea et al., 2016). Points and boxplots are colored by climate zone (T, tundra; S, subarctic; HC, humid continental; TO, temperate oceanic).

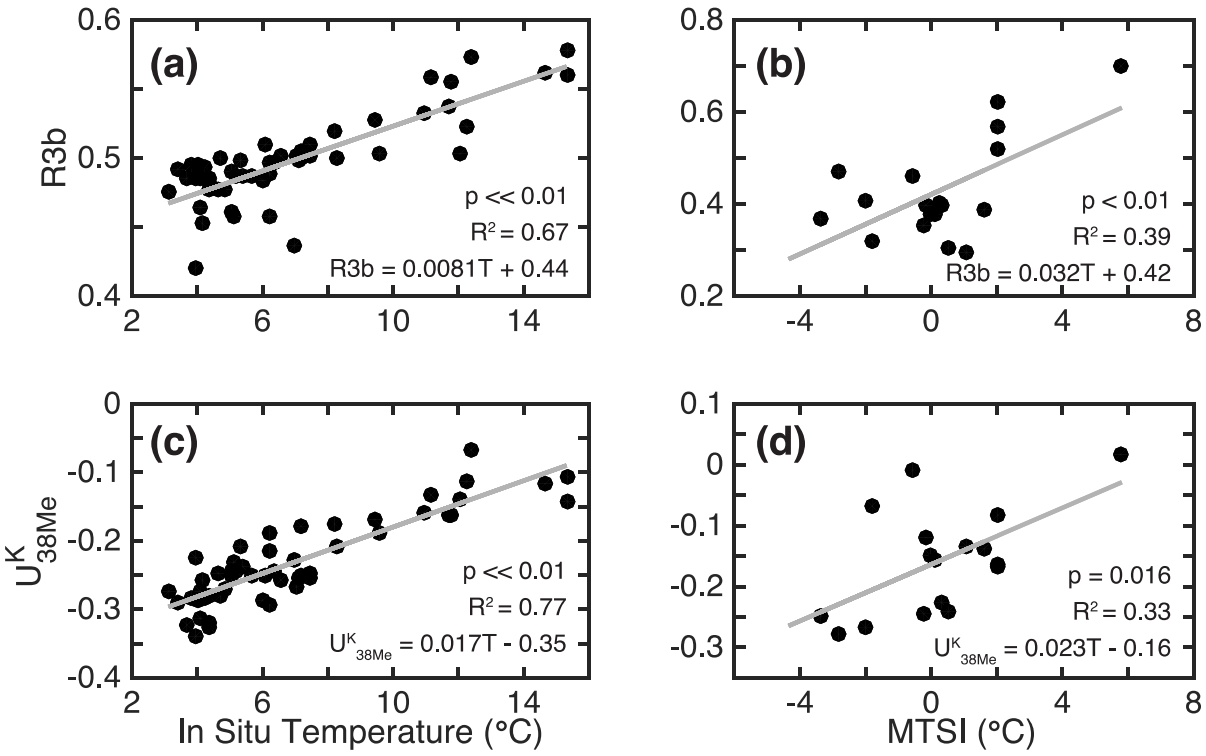

945 **Fig. 7.** (a) 3b isomer ratio (R3b) vs. *in situ* temperature from the Toolik Lake calibration (Longo et al., 2016). The strong positive correlation demonstrates the potential for use of R3b as a temperature proxy. (b) The Northern Hemispheric lakes dataset also shows a significant positive correlation between R3b and MSTI. (c) U^{K}_{38Me} vs. *in situ* temperature from the Toolik Lake calibration (Longo et al., 2016) and (d) U^{K}_{38Me} vs. MTSI from the
950 Northern Hemispheric lakes dataset.

Table 1. Lakes and samples analyzed in this study with water chemistry and LCA distribution parameters.[1]

ID	Lake Name	Lat.	Long.	Sample Type	pH	Salinity classification	LCA Occurrence/ Distribution	U^{K}_{37}	RIK_{37}	RIK_{38E}	C_{37}/C_{38}	$\%C_{37:4}$
G-01	Baejarvotn	65.73	-21.43	core	7.4	fresh	Group I	-0.27	0.49	0.33	1.22	35.09
G-02	Breiter Luzin	53.35	13.46	SS	8.7	fresh	Group I	-0.45	0.64	0.48	1.53	49.50
G-03	Erlongwan	42.30	126.38	SS	8.7	fresh	Group I	-0.35	0.56	0.27	1.06	45.35
G-04	Étang des Vallées	48.69	1.92	SS	7.2	fresh	**Group I†**	-0.32	0.60	0.57	1.54	36.47
G-05	Feldberger Haussee	53.35	13.45	SS	8.9	fresh	Group I	-0.40	0.63	0.40	1.19	46.69
G-06	Hajeren	79.26	11.52	core	6.6	fresh	Group I	-0.42	0.54	0.00	1.02	49.09
G-07	Hakluytvatnet	79.77	10.74	core	5.9	fresh	Group I	-0.60	0.49	0.15	1.03	62.18
G-08	Hakluytvatnet	79.77	10.74	core	5.9	fresh	Group I	-0.62	0.51	0.11	0.94	63.19
G-09	Ichi-no-Megata	39.95	139.74	SPM	7.2	fresh	Group I	-0.47	0.60	0.33	1.38	52.70
G-10	Ichi-no-Megata	39.95	139.74	SPM	7.2	fresh	Group I	-0.48	0.59	0.44	3.33	53.61
G-11	Lake Toyoni	42.09	143.27	SS	7.2	fresh	**Group I†**	-0.48	0.54	0.17	0.84	51.06
G-12	Schmaler Luzin	53.32	13.44	SS	8.5	fresh	Group I	-0.42	0.63	0.45	1.39	46.02
G-13	Skufnavotn	65.89	-22.12	core	ND	fresh	Group I	-0.45	0.48	0.15	0.69	49.24
G-14	Svartagilsvatn	65.85	-21.88	core	ND	fresh	Group I	-0.59	0.55	0.08	0.75	63.39
G-15	Upper Murray Lake	81.33	-69.50	core	8.2	fresh	**Group I†**	-0.55	0.57	0.30	0.88	59.83
G-16	Vatnsdalsvatn	65.61	-23.11	core	6.7	fresh	Group I	-0.63	0.58	0.16	0.94	62.91
G-17	Vestre Gisholtsvatn	63.95	-20.52	core	7.7	fresh	Group I	-0.57	0.60	0.23	0.97	57.29
G-18	Vikvatnet	68.20	13.58	ST	7.0	fresh	**Group I†**	-0.25	0.60	0.48	1.07	32.10
G-19	Wudaliangchi	48.73	126.17	SS	7.8	fresh	Group I	-0.49	0.60	0.15	1.08	55.00
G-20	Xianhe	47.36	120.45	SS	7.8	fresh	Group I	-0.39	0.54	0.25	0.98	45.33
G-21	Khirgis Nuur	49.20	93.40	SS	9.4	mesohaline	Group II	0.20	1.00	1.00	3.43	0.00
G-22	Yarkov Basin of Chany Lake	54.94	77.98	core	7.2	mesohaline	Group II	0.25	1.00	1.00	0.98	0.00
G-23	Yarkov Basin of Chany Lake	54.94	77.98	core	7.2	mesohaline	Mixed I/II	-0.18	0.76	0.52	1.23	34.11
G-24	Airag Nuur	48.90	93.47	SS	9.6	mesohaline	ND					
G-25	Baejarvotn	65.73	-21.43	core	7.4	fresh	ND					
G-26	Haukadalsvatn	65.05	-21.63	core	7.7	fresh	ND					
G-27	Hestvatn	64.01	-20.72	core	7.8	fresh	ND					
G-28	Hestvatn	64.01	-20.72	core	7.8	fresh	ND					
G-29	Hvitarvatn	64.60	-19.83	core	7.5	fresh	ND					
G-30	Hvitarvatn	64.60	-19.83	core	7.5	fresh	ND					
G-31	Kotuvatn	66.06	-21.87	core	ND	fresh	ND					
G-32	Lake Mongco	29.53	98.84	core	ND	fresh	ND					
G-33	Laugabolsvatn	65.98	-22.67	core	7.6	fresh	ND					
G-34	Longhupao	46.72	124.38	SS	8.4	fresh	ND					
G-35	Small Chany Lake	54.55	77.98	core	8.9	oligohaline	ND					
G-36	Small Chany Lake	54.55	77.98	core	8.9	oligohaline	ND					
G-37	Wuliangsuhai	40.82	108.85	SS	7.8	oligohaline	ND					

955

Table 2. Phylotype mixing model results from three samples with mixed Group I/II distributions.

Sample	Salinity (psu)	RIK_{37}	Group I (% contribution)[1]	Group II (% contribution)[1]	Reference
Yarkov Basin (32.5 cm)[2]	unknown (modern = 6)	0.76	54.5 ± 1.55	45.4 ± 1.55	This study; Song et al., 2016b
Shannon Lake	2.4	0.69	70.4 ± 2.01	29.5 ± 2.01	Toney et al., 2011; Longo et al., 2016
Humboldt Lake	1.5	0.78	50.0 ± 1.42	50.00 ± 1.42	Toney et al., 2011; Longo et al., 2016